RESEARCH MEMORANDUM

AERODYNAMIC CHARACTERISTICS IN PITCH OF SEVERAL TRIPLE-BODY MISSILE CONFIGURATIONS AT MACH NUMBERS FROM 0.6 TO 1.4

By Earl D. Knechtel and Arvid N. Andrea

Ames Aeronautical Laboratory
Moffett Field, Calif.

NATIONAL ADVISORY COMMITTEE
FOR AERONAUTICS

WASHINGTON
November 2, 1956
Declassified January 12, 1961

NATIONAL ADVISORY COMMITTEE FOR AERONAUTICS

RESEARCH MEMORANDUM

AERODYNAMIC CHARACTERISTICS IN PITCH OF SEVERAL TRIPLE-BODY MISSILE CONFIGURATIONS AT MACH NUMBERS FROM 0.6 TO 1.4

By Earl D. Knechtel and Arvid N. Andrea

SUMMARY

An experimental investigation was conducted to determine the longitudinal aerodynamic characteristics at transonic speeds of missile configurations having three blunted cone-cylinder bodies. Modifications of the basic model were tested to indicate the effects of (a) relative lengths of coplanar bodies, (b) seals between the cylindrical portions of the bodies, (c) horizontal connecting surfaces near the rear of the bodies, and (d) triangular rather than coplanar body grouping. Lift, drag, and pitching-moment data were obtained at angles of attack from -4° to $+12^{\circ}$ and Mach numbers from 0.6 to 1.4 for a constant Reynolds number of 5.5×10^{6}, based on average body length.

Results of the investigation indicate that all configurations had centers of pressure well ahead of the centroid of plan-form area. Effects of Mach number variation on lift and center of pressure were generally slight. The principal effect of relative body length was a systematic reduction in wave drag with increased slenderness. The addition of seals caused a slight forward movement of the center of pressure. The addition of horizontal surfaces between bodies had completely detrimental effects on lift, drag, and center-of-pressure characteristics. Change to a triangular body grouping caused large reductions in lift and a slight forward shift in center of pressure.

Comparison of experimental results with available theory indicates that a combination of slender-wing and viscous-crossflow theories is satisfactory for estimating the lift of these triple-body missile configurations but inadequate for estimating pitching moments.

INTRODUCTION

In recent years, intensified missile research resulting from increased interest in that field has made available large amounts of aerodynamic data for ballistic-missile configurations through a wide range of Mach numbers. These configurations generally have been fin-stabilized bodies of revolution, which, in actual use as ballistic missiles, would achieve long range by employing multiple rocket stages in series along the body. A second approach to the design of long-range missiles which is being considered differs from the conventional approach in two main aspects. These are first, that stability and control would be provided by servo-control of the rocket thrust axes, and second, that the first rocket stage would utilize the rocket motor in the central, or second-stage, body as well as rocket motors in parallel side bodies. The side bodies would supply fuel for all motors until the end of the first stage, when they would be jettisoned.

Calculations (ref. 1) indicate that, as compared with a conventional tandem-staged rocket design having the same weights of structure, fuel, and payload, the lateral-staging arrangement offers a higher effective thrust-to-weight ratio and greater reliability in firing. Possible disadvantages from a practical standpoint, however, are the higher drag and greater peak acceleration of the multiple-body missile.

The scarcity of data on configurations of this type leaves unanswered such questions as how the lift, drag, and center of pressure vary with Mach number and angle of attack, how these characteristics compare with those of a single body of revolution, and whether existing methods of calculating potential and viscous loads may be utilized in the present case with sufficient accuracy for engineering purposes. In order to obtain answers to these questions, the present investigation was conducted to determine the longitudinal aerodynamic characteristics at transonic speeds of a related set of missile configurations consisting of three similar bodies. These bodies were arbitrarily chosen as blunted cone-cylinders. The design variables investigated were relative body length, seals between bodies, horizontal surfaces at the rear of the bodies, and triangular rather than coplanar grouping of the bodies.

NOTATION

b	model span
C_D	drag coefficient, $\frac{\text{drag}}{qS}$
$C_{D_{min}}$	minimum drag coefficient

C_L lift coefficient, $\frac{\text{lift}}{qS}$

C_m pitching-moment coefficient, $\frac{\text{pitching moment}}{qSd}$

d body diameter

L lift

$\left(\frac{L}{D}\right)_{max}$ maximum lift-drag ratio

M free-stream Mach number

q free-stream dynamic pressure

S base area of model

α angle of attack, deg

Model Designations

1 coplanar bodies of equal length

2 coplanar bodies, center body short

3 coplanar bodies, center body long

4 triangular grouping of equal-length bodies

H horizontal connecting surfaces at rear of bodies

S seals between cylindrical bodies

MODELS AND APPARATUS

The investigation was conducted in the Ames 2- by 2-foot transonic wind tunnel. This facility, described in detail in reference 2, has a ventilated test section which allows continuous choke-free operation through the range of Mach numbers up to 1.4.

The eight triple-body model configurations are shown in figure 1. Each had three parallel bodies which were cone-cylinders 1.50 inches in diameter, connected by modified-wedge struts across the 0.10-inch gap between bodies. For seven of the models, the parallel body axes were coplanar, whereas the bodies of the remaining configuration were arranged

in a more compact triangular grouping. The identical nose cones were derived from a basic cone of fineness ratio 4 which was truncated and made 20 percent blunt by the addition of a hemispherical nose, in accordance with the results of recent investigations of drag and aerodynamic heating of cone-cylinders (refs. 3 and 4).

The relative body lengths of models 1, 2, and 3 were chosen so as to maintain constant total volume and surface area. Models 1S, 2S, and 3S comprised a corresponding set for which the gaps between cylinders were sealed. Model 1H differed from model 1 only in the horizontal connecting surfaces added at the rear of the bodies. In addition, limited tests were made of an individual body of configuration 1.

The models were mounted in the test section on a sting-supported internal strain-gage balance, as shown in figure 2.

TESTS AND DATA REDUCTION

Lift, drag, and pitching moment were measured for all models through an angle-of-attack range from -4° to $+12^{\circ}$ at ten Mach numbers (0.6, 0.8, 0.9, 0.94, 0.98, 1.02, 1.06, 1.1, 1.2, and 1.4). A constant Reynolds number of 5.5×10^{6}, based on average body length, was maintained throughout the tests.

All coefficients were referred to the total base area, and the reference length for the pitching-moment coefficients was one body diameter. The pitching moments were taken about the centroid of plan-form area of configuration 1 (6.32 in. ahead of the base of the center body), this centroid location differing only slightly from those of the other configurations tested. Angles of attack were defined as lying in the plane of symmetry perpendicular to the common plane of the two outer body axes.

Corrections were applied to the angles of attack to account for deflections of the sting and balance under static aerodynamic loads, and to the drag to adjust for the difference between measured base pressures and free-stream static pressure.

Subsonic wall-interference corrections calculated by the method of reference 5 were found to be small enough to neglect for the present models, which blocked as much as 0.9 percent of the cross-sectional area of the test section. No corrections were made for possible wall interference caused by reflected shock waves at low supersonic speeds. Corrections for drag buoyancy and air-stream angularity were unnecessary since they were known to be less than the probable errors in measuring drag and angle of attack, respectively.

Apart from the systematic errors caused by neglecting the above corrections, a root-mean-square analysis of scatter shows that the data are correct within the following random errors of measurement:

$$M \pm 0.003$$

$$\alpha \pm 0.03^{\circ}$$

$$C_L \pm 0.040$$

$$C_D \pm 0.008$$

$$C_m \pm 0.13$$

RESULTS AND DISCUSSION

The three-body arrangements of the present report showed only a minor effect of Mach number on the variations of lift, drag, and pitching moment with angle of attack. For this reason, the general effects of angle of attack on the coefficients of lift, drag, and pitching moment are shown by presenting variations of the coefficients with angle of attack for only three of the ten Mach numbers investigated. In order to provide a more detailed indication of the effects of configuration geometry on the longitudinal characteristics, values of lift parameter C_L/α (taken equal to $dC_L/d\alpha$ at $\alpha = 0^{\circ}$), center of lift, minimum drag coefficient, and maximum lift-drag ratio are shown as functions of Mach number.

The variations of coefficients of lift, drag, and pitching moment with angle of attack at the selected Mach numbers are given in figure 3. These data are for the five unsealed configurations; however, the shapes of these curves are representative of those for the corresponding sealed configurations. Note that when effects of relative length and grouping of bodies are present, they are indicated not so much by changes in the shapes of the curves as by changes in the slopes of the lift and pitching-moment curves and by shifts in the drag curves.

Values of lift parameter, center of pressure, minimum drag coefficient, and maximum lift-drag ratio for all eight configurations are presented in figures 4 to 7 as functions of Mach number. Maximum lift-drag ratio, although not in itself a significant parameter for a true ballistic missile, is shown here as a measure of relative lifting efficiency, since some of the present configurations were found to have values of maximum lift-drag ratio not far below those of existing or proposed supersonic airplanes and glide missiles. These results indicate that certain characteristics were common to all configurations tested. For instance, all configurations had centers of lift located from 12 to 25 percent of body length ahead of the plan-form-area centroid and therefore, in actual use,

would require the addition of stabilizing surfaces, servo-directed thrust lines, or other means of stabilization in flight. Another result common to all eight models was the generally small variation of lift parameter C_L/α and center of pressure with Mach number, whereas minimum drag coefficient and maximum lift-drag ratio had moderate to large variations with Mach number, depending upon the configuration. Effects of specific configuration changes are discussed in more detail in the sections which follow.

Effects of Relative Body Length

Examination of figures 4 to 7 indicates that relative body length, or axial disposition of model volume, had an important effect only on minimum drag. Results shown in figure 6 for both sealed and unsealed coplanar models indicate that, although the subsonic drag levels were the same for the three nose arrangements, the transonic drag rise with Mach number was greatest for the least slender configurations, 1 and 1S, and the supersonic wave drag was progressively reduced by as much as 45 percent for the more slender models. This result is, of course, in accord with existing area-rule concepts (ref. 6) which have shown that at Mach numbers near unity the drag rise of a slender body or wing-body combination may be reduced by making the longitudinal distribution of cross-sectional area more smooth and gradual. In order to compare the present models on this basis, the longitudinal development of cross-sectional area is shown in figure 8 for the basic configurations, together with the optimum, or Sears-Haack, area distribution for a body having the same volume, base area, and length as configuration 3. This comparison indicates that, although configuration 3 had the most favorable area distribution of the present models, further drag reductions could be realized by a closer approximation to the optimum.

Goethert (ref. 7) has shown that perforated walls of the type employed in this case not only fail to cancel strong expansion waves originating at the shoulders of cone-cylinders, but instead reflect them as compression waves back to the model. Incompletely attenuated waves of this type are believed to have caused the deviations in lift parameter and center of pressure shown in figures 4 and 5 for some of the models at Mach numbers from 1.0 to 1.1. Aside from this extraneous effect, which was generally least for the more slender configurations, relative body length had only minor effects on lift and center of pressure. For the basic nose arrangements of configurations 1, 2, and 3, center-of-pressure travel over the Mach number range from 0.6 to 1.4 did not exceed 5 percent of the body length.

To determine values of maximum lift-drag ratio for certain models and Mach numbers of those shown in figure 7, slight extrapolations were necessary when the maximum lift-drag ratio did not occur within the angles of attack investigated. For all except the lowest Mach numbers tested, the

maximum lift-drag ratios were significantly affected by relative body length and became progressively larger with increased slenderness. That this result can be attributed largely to the systematic effect of slenderness on minimum drag noted previously becomes apparent when the maximum lift-drag ratio is expressed in terms of minimum drag coefficient and lift parameter as

$$\left(\frac{L}{D}\right)_{max} = \frac{\sqrt{57.3}}{2}\sqrt{\frac{C_{L_\alpha}}{C_{D_{min}}}} \qquad (\alpha \text{ in deg})$$

This expression is for the case of zero leading-edge suction, which the experimental results indicated to be approximately the case for the present configurations.

Effects of Seals Between Bodies

The principal effect of adding seals to any of the three basic models was a slight to moderate forward movement of the center of pressure (see fig. 5) throughout the Mach number range from 0.6 to 1.4. This undesirable increase of instability became slightly less pronounced as the angle of attack was increased.

Seals were found to cause relatively little change in lift (fig. 4), indicating the predominant effects of viscosity in reducing the flow through the narrow unsealed gaps. Corresponding sealed and unsealed configurations also had practically identical values of minimum drag coefficient, as indicated in figure 6 and, as a result, values of maximum lift-drag ratio (fig. 7) were not changed significantly by sealing the gaps between bodies.

Effects of Horizontal Surfaces Between Bodies

When horizontal connecting surfaces were added near the rear of the bodies, the main effect was a large increment in minimum drag coefficient throughout the Mach number range, as indicated in the lower part of figure 6 for configurations 1 and 1H. These results indicate the occurrence, even at moderate subsonic Mach numbers, of choked flow between the horizontal surfaces (see section B-B, fig. 1(a)). This choking phenomenon, in combination with the horizontal struts themselves, produced over the rear portion of model 1H the discontinuous increase of cross-sectional area shown in figure 8 and caused the drag level of this configuration to be the highest obtained in the investigation.

Addition of horizontal surfaces also caused reductions in lift parameter (fig. 4) as large as 20 percent and forward shifts in center of pressure (fig. 5) as great as 20 percent of body length. These effects, which accompanied the growth of shock waves on the horizontal surfaces, were greatest at zero angle of attack and at high subsonic Mach numbers, but diminished at larger angles of attack as the upper surface became immersed in the wake of the body.

As a result of the increased minimum drag coefficient of configuration 1H, the maximum lift-drag ratios of that configuration (fig. 7) were reduced by as much as 25 percent from those of configuration 1. The reduction was greatest at subsonic Mach numbers, where the relative drag increase was largest.

Effects of Triangular Body Grouping

Grouping of the bodies in a triangular rather than coplanar pattern reduced the lift parameter (fig.4) to approximately 40 percent of that for configuration 1. For later reference, it is worth noting that this ratio of lifts for configurations 1 and 4 is approximately the square of the ratio of model spans.

The center of pressure of configuration 4 was from 5 to 15 percent of body length ahead of that of configuration 1, the difference being greatest at supersonic speeds and at small angles of attack. Except in the range of Mach numbers between 0.8 and 1.0, the center of pressure of configuration 4 was the farthest forward of all the configurations investigated. However, the actual pitching moment required to be trimmed out at any given Mach number and angle of attack was less than that of any other triple-body configuration.

The maximum lift-drag ratio (fig. 7) of configuration 4 was much lower at all Mach numbers than that of any other triple-body model tested, and was approximately 60 percent as great as that of coplanar configuration 1. This reduction in lift-drag ratio is attributable almost entirely to the reduced lift.parameter (greater drag due to lift) of model 4, inasmuch as only slight differences in minimum drag are shown in figure 6 for the two models.

Comparison With Available Theory

As with more conventional configurations, it is of interest to know how well the experimental results agree with results obtained by available theoretical methods. No exact solution is known to have been obtained for the potential flow about lifting multiple-body configurations of the type

being investigated here. For this reason, the calculated values of lift and pitching moment presented here were obtained by applying the most nearly applicable approximate potential theories in combination with viscous crossflow theory, as has been done for bodies of revolution (ref. 8) and low-aspect-ratio wings (ref.9).

The two potential theories considered were the slender-wing theory of reference 10 and the slender-body theory of reference 11. These two methods indicate, respectively, probable upper and lower limits of the theoretical lift, depending upon whether these triple-body missile configurations are approximated by a composite slender wing having the same span as the given model or by three noninterfering cone-cylinders. In the present case, values of potential lift obtained by the slender-wing theory are as much as three times as great as the lift of three independent slender bodies. However, it is of interest to note that a slender body of revolution with a cylindrical afterbody has the same potential lift as that of a slender wing whose span, b, is equal to the diameter of the body of revolution. This lift would be given by either reference 10 or 11 as

$$L = \frac{\pi^2}{360} b^2 q\alpha \quad (\alpha \text{ in deg})$$

Because favorable pressure gradients might be expected to forestall flow separation on the nose cones, viscous crossforces were assumed to act only on the cylindrical portions of the models. For these calculations, the two-dimensional drag coefficients given in reference 12 were corrected for finite cylinder length as in reference 8. The calculated values thus indicate the effects of viscous crossflow in combination with each of the two potential theories mentioned above.

In figure 9, representative lift and pitching-moment results are compared with calculated values for models 1 and 4. First, with respect to the lift curves, the comparison indicates good agreement of the slender-wing theory with experiment for both configurations 1 and 4. However, when the potential lift was calculated for three noninterfering slender bodies, the lift was underestimated by approximately two thirds for model 1 and to a lesser degree for model 4.

To aid in examining these differences, experimental coefficients of lift and pitching moment are shown in figure 9(a) for a single cone-cylinder identical to the bodies of models 1 and 4. These experimental results agree reasonably well with the calculated slender-body coefficients, and both apply equally well to one body or to three noninterfering bodies. The large differences between the experimental lift curves for the single body and the triple body then indicate that interference between bodies caused approximately two thirds of the lift of model 1. As shown previously, the lift of model 1 was underestimated to approximately that extent by the slender-body theory when interference was neglected, whereas the calculated lift of a composite slender wing agreed well with the measured lift of model 1.

Comparisons of experimental and calculated pitching moments for the triple-body models did not show the same trends as did the lift curves. When configuration 1 was approximated by a composite triangular wing, the pitching moments calculated by slender-wing theory were about 50 percent higher than the experimental values, as indicated in figure 9(a). However, when the model was approximated by three noninterfering cone-cylinders, the calculated pitching moments were approximately 50 percent below the experimental values for model 1, but in good agreement with the experimental single-body results. For model 4, as shown in figure 9(b), the tendency again is for the slender-wing theory to yield pitching-moment values too high, and for slender-body theory to give values too low when interference is neglected. However, the discrepancies are much less in this case.

It is apparent that available theories do not adequately describe the load distribution on multiple-body missile configurations of the present type. This is particularly true of the effects of mutual interference between bodies.

CONCLUSIONS

The results of this experimental investigation of the aerodynamic characteristics in pitch of several triple-body missile configurations lead to the following conclusions:

1. All triple-body configurations tested had centers of pressure well ahead of the centroid of plan-form area. Effects of Mach number on lift and center of pressure were generally slight.

2. For models having coplanar body axes, the principal effects of relative body length were systematic reductions in wave drag of as much as 45 percent and corresponding increases in maximum lift-drag ratio with increasing slenderness.

3. The only significant effect of sealing the gap between bodies was a slight forward shift in the center of pressure.

4. Addition of horizontal connecting surfaces near the rear of the bodies had entirely detrimental effects, including a large drag increment throughout the Mach number range, decreased lift, and a forward shift in center of pressure of as much as 20 percent of body length.

5. Grouping of the three bodies in a triangular rather than coplanar pattern resulted in a 60-percent reduction in lift, a 40-percent reduction in maximum lift-drag ratio, and a slight forward shift in center of pressure.

6. Comparison of experimental results with available theory indicates that a combination of slender-wing and viscous-crossflow theory provides a satisfactory estimate of the lift of these triple-body missiles, but not of the pitching moment.

Ames Aeronautical Laboratory
National Advisory Committee for Aeronautics
Moffett Field, Calif., Aug. 31, 1956

REFERENCES

1. Cole, Dandridge M., and Epstein, L. Ivan: Interpretation of the Malina-Summerfield Criterion for Optimization of Multistage Rockets. Jour. American Rocket Society, vol. 26, no. 3, Mar. 1956, p. 188.

2. Spiegel, Joseph M., and Lawrence, Leslie F.: A Description of the Ames 2- by 2-Foot Transonic Wind Tunnel and Preliminary Evaluation of Wall Interference. NACA RM A55I21, 1956.

3. Sommer, Simon C., and Stark, James A.: The Effect of Bluntness on the Drag of Spherical-Tipped Truncated Cones of Fineness Ratio 3 at Mach Numbers 1.2 to 7.4. NACA RM A52B13, 1952.

4. Allen, H. Julian, and Eggers, A. J., Jr.: A Study of the Motion and Aerodynamic Heating of Missiles Entering the Earth's Atmosphere at High Supersonic Speeds. NACA RM A53D28, 1953.

5. Baldwin, Barrett S., Turner, John B., and Knechtel, Earl D.: Wall Interference in Wind Tunnels with Slotted and Porous Boundaries at Subsonic Speeds. NACA TN 3176, 1954. (Formerly NACA RM A53E29)

6. Whitcomb, Richard T.: A Study of the Zero-Lift Drag-Rise Characteristics of Wing-Body Combinations Near the Speed of Sound. NACA RM L52H08, 1952.

7. Goethert, B. H.: Physical Aspects of Three-Dimensional Wave Reflections in Transonic Wind Tunnels at Mach No. 1.20 (Perforated, Slotted, and Combined Slotted-Perforated Walls). Arnold Engineering Development Center TR 55-45, Mar. 1956.

8. Allen, H. Julian, and Perkins, Edward W.: Characteristics of Flow over Inclined Bodies of Revolution. NACA RM A50L07, 1951.

9. Flax, A. H., and Lawrence, H. R.: The Aerodynamics of Low-Aspect-Ratio Wings and Wing-Body Combinations. Rep. CAL-37, Cornell Aero. Lab. Inc., Sept. 1951.

10. Jones, Robert T.: Properties of Low-Aspect-Ratio Pointed Wings at Speeds Below and Above the Speed of Sound. NACA Rep. 835, 1946.

11. Tsien, Hsue-Shen: Supersonic Flow Over an Inclined Body of Revolution. Jour. Aero. Sci., vol. 5, no. 12, Oct. 1938, pp. 480-483.

12. Delaney, Noel K., and Sorenson, Norman E.: Low-Speed Drag of Cylinders of Various Shapes. NACA TN 3038, 1953.

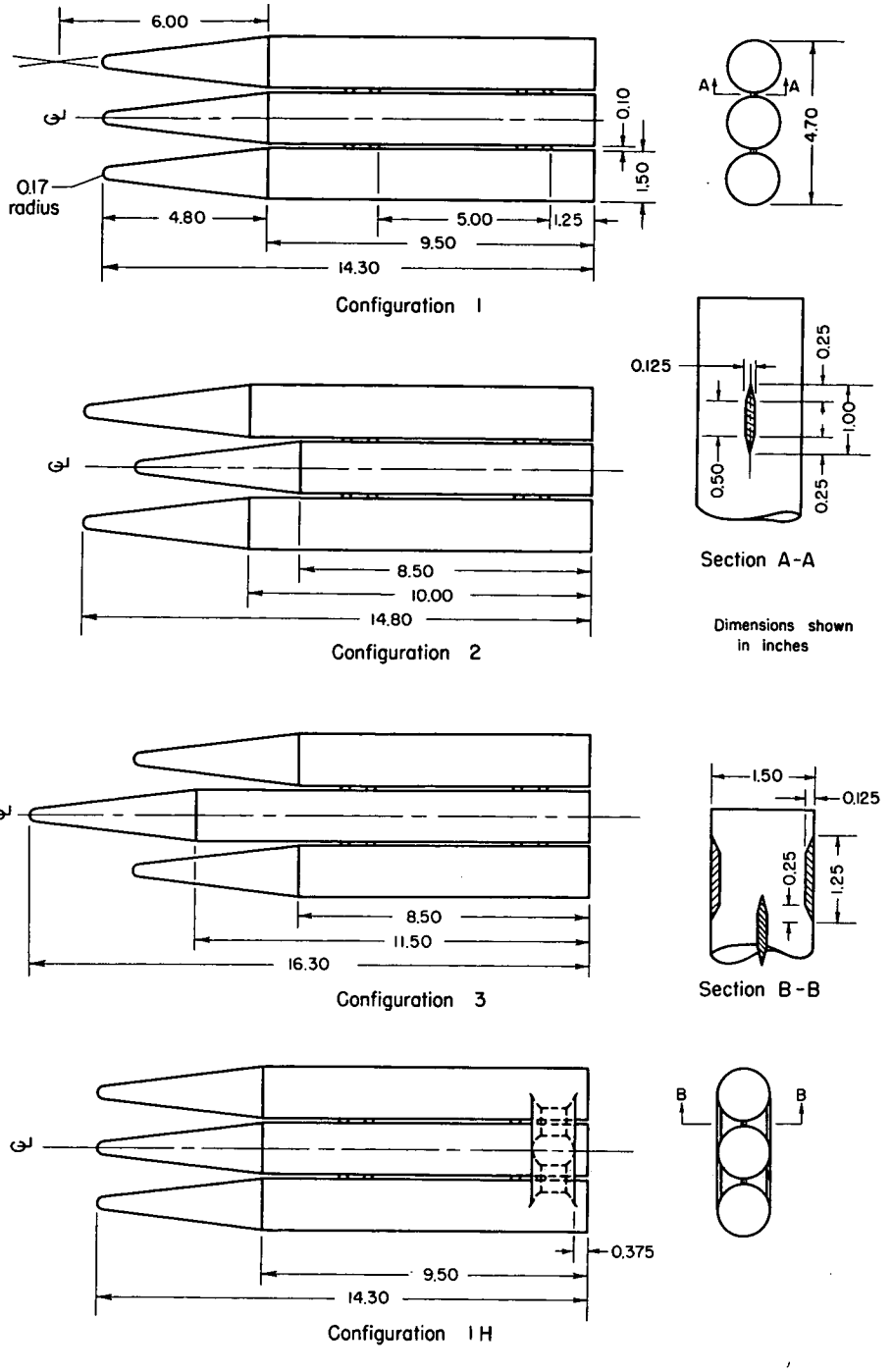

(a) Configurations 1, 2, 3, and 1H.

Figure 1.- Plan forms of models and geometric details.

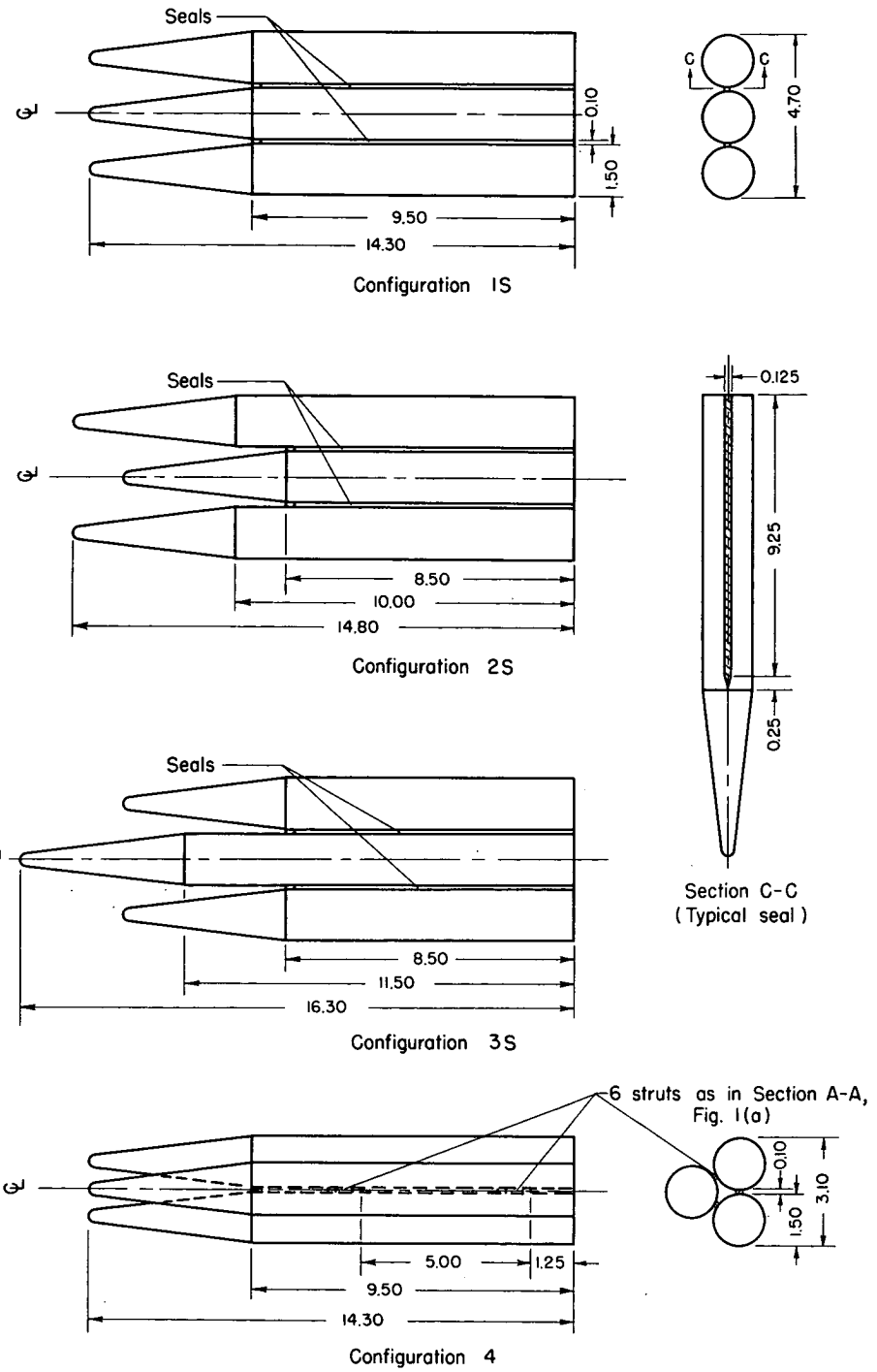

(b) Configurations 1S, 2S, 3S, and 4.

Figure 1.- Concluded.

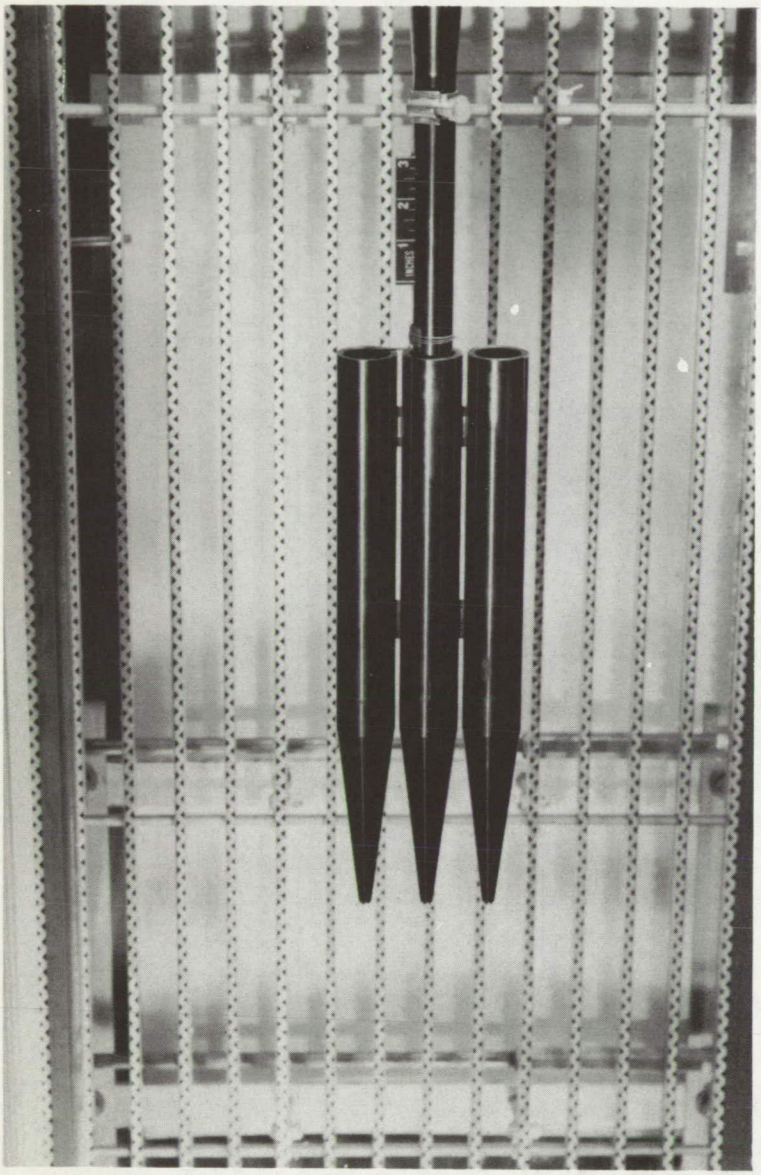

Figure 2.- Typical model installed in the Ames 2- by 2-foot transonic wind tunnel.

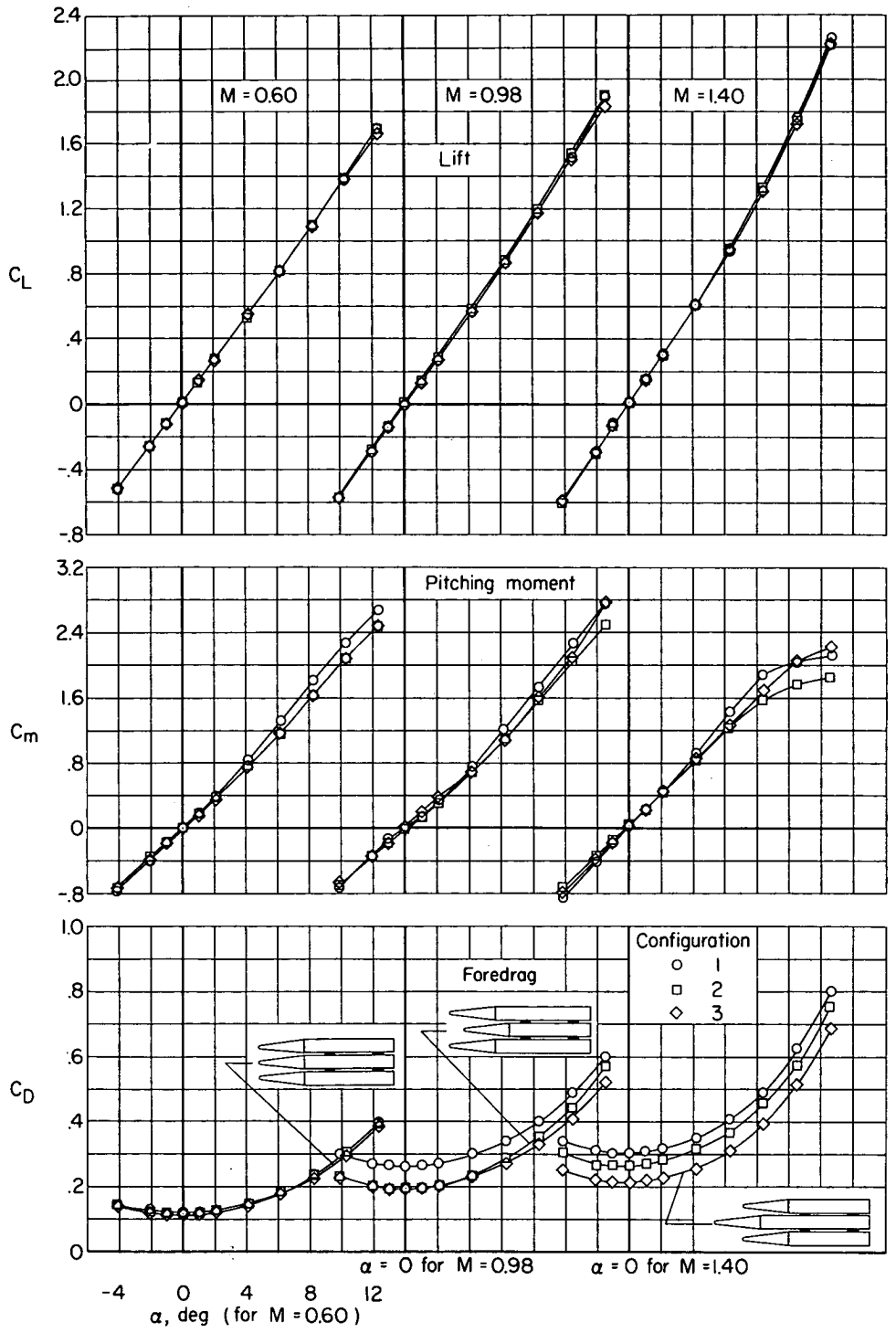

(a) Configurations 1, 2, and 3.

Figure 3.- Typical aerodynamic characteristics of several triple-body missile configurations.

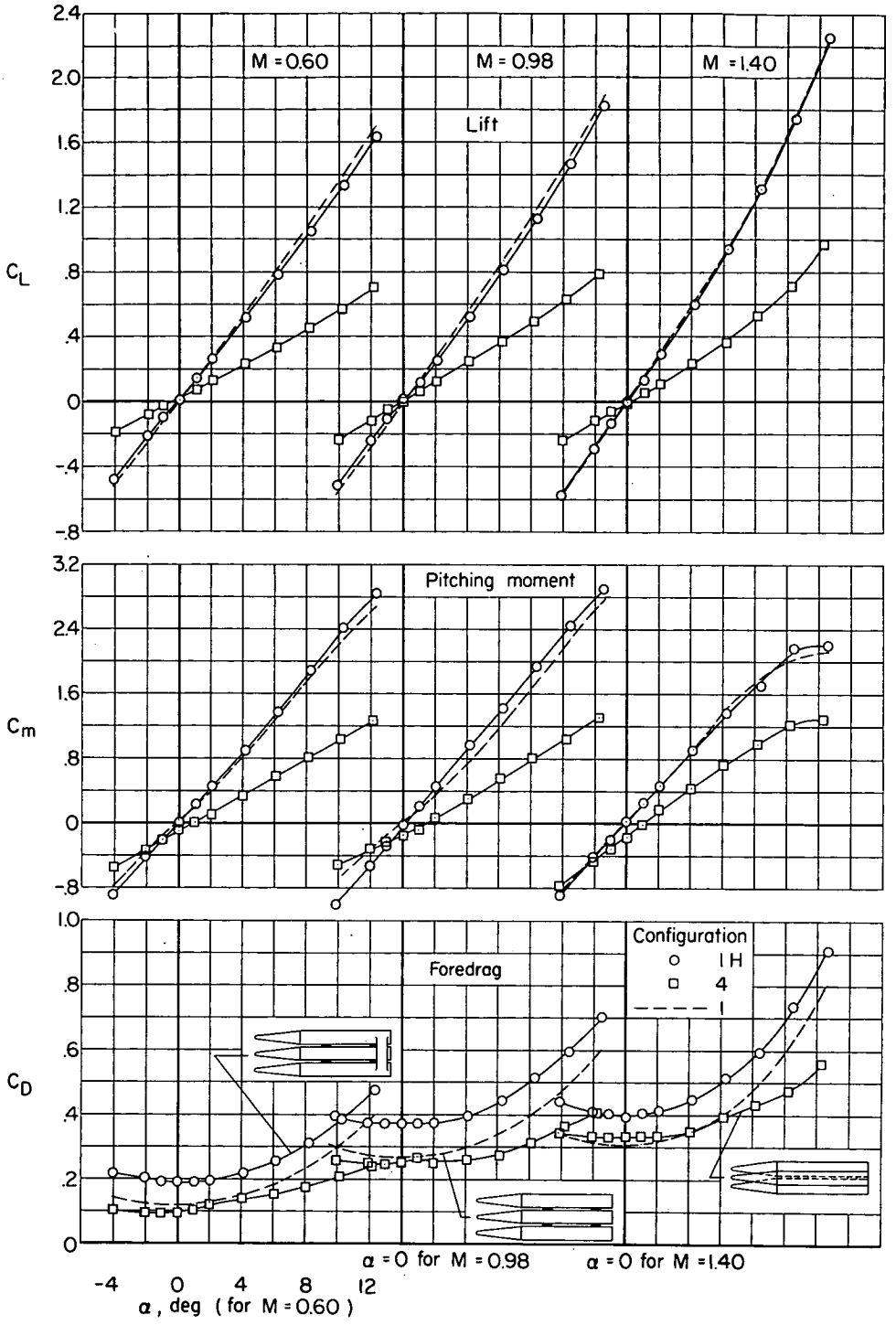

(b) Configurations 1H and 4.

Figure 3. - Concluded.

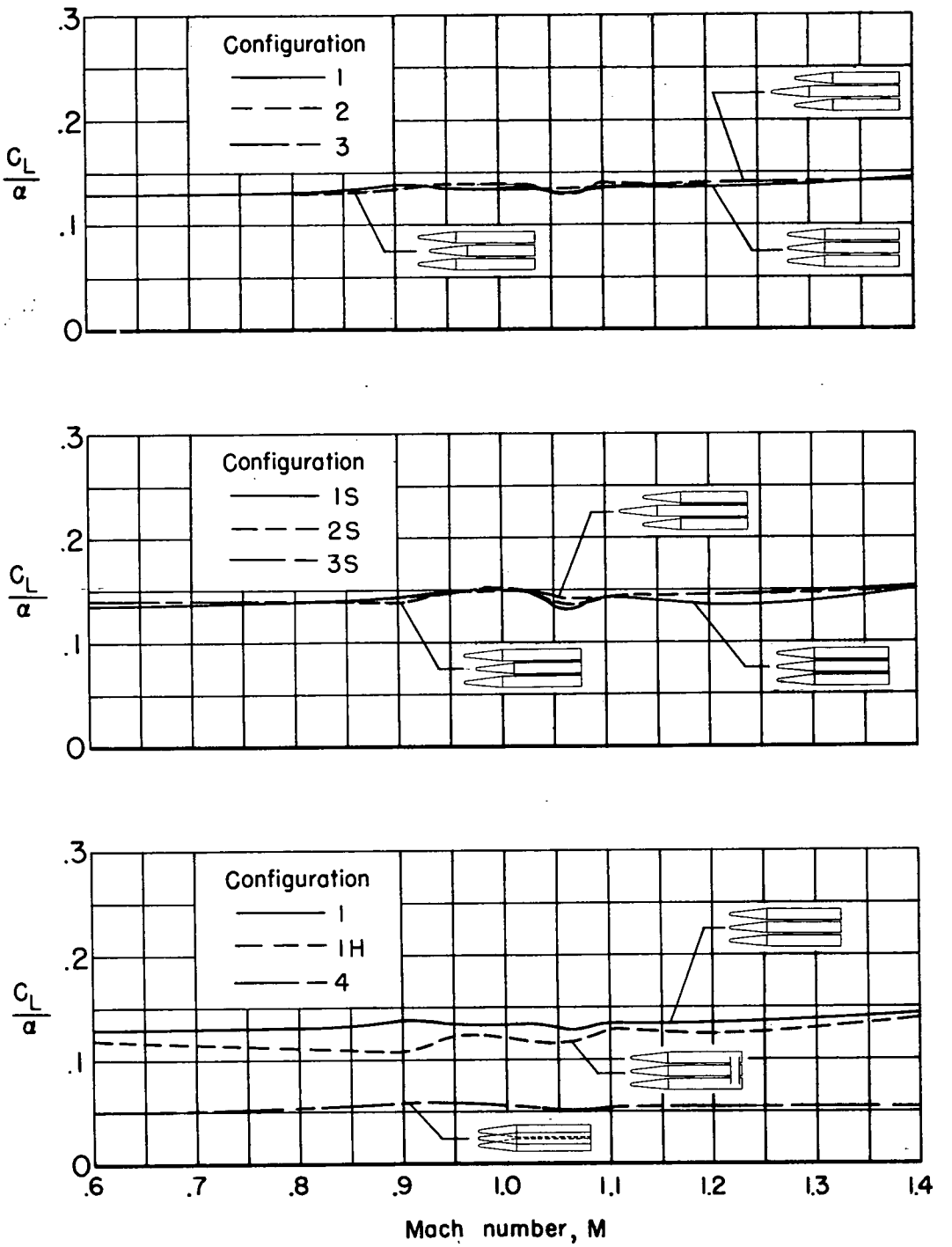

(a) $\alpha = 0°$

Figure 4. – Variation of lift parameter with Mach number for several triple–body missile configurations.

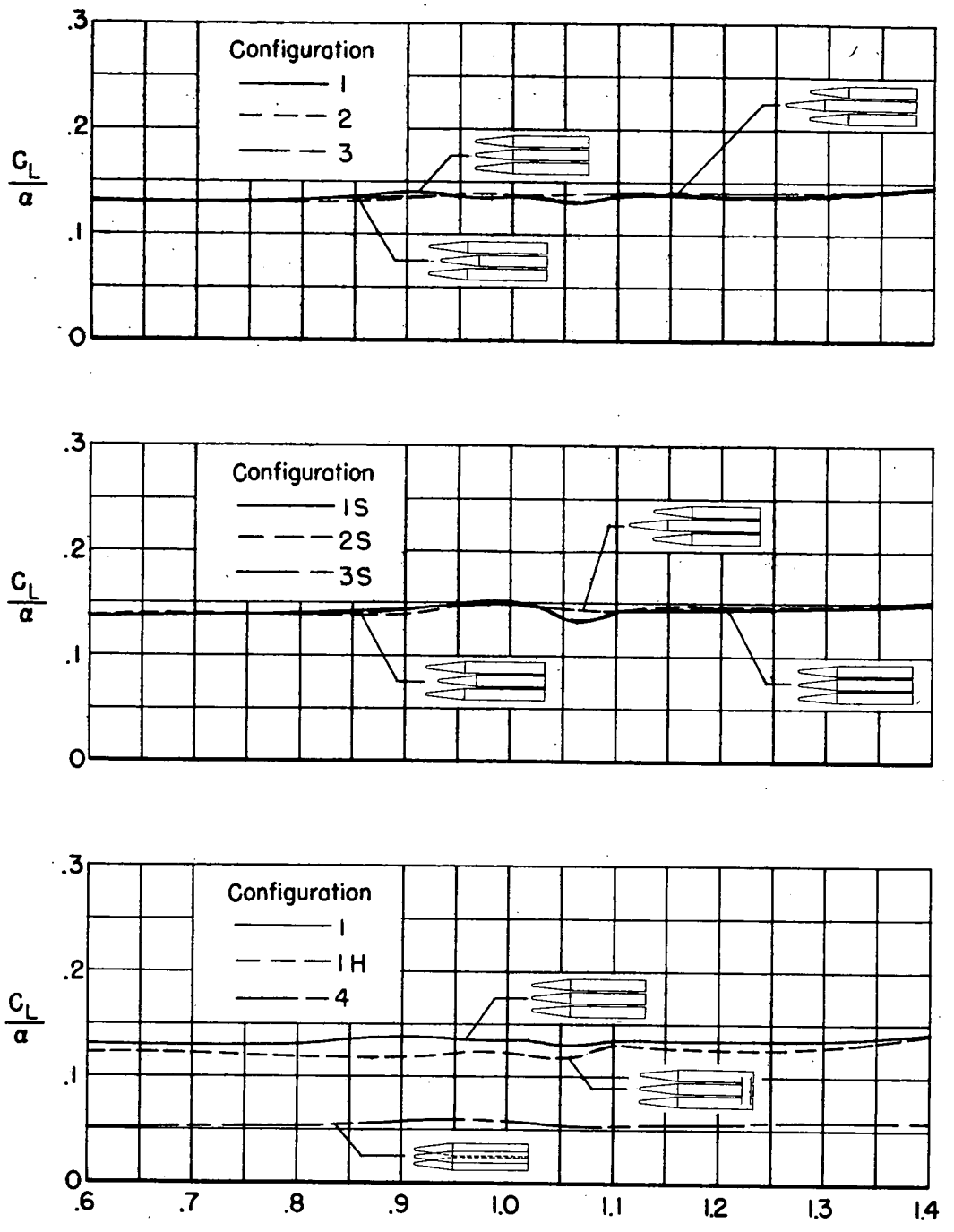

(b) $\alpha = 4°$

Figure 4. – Continued.

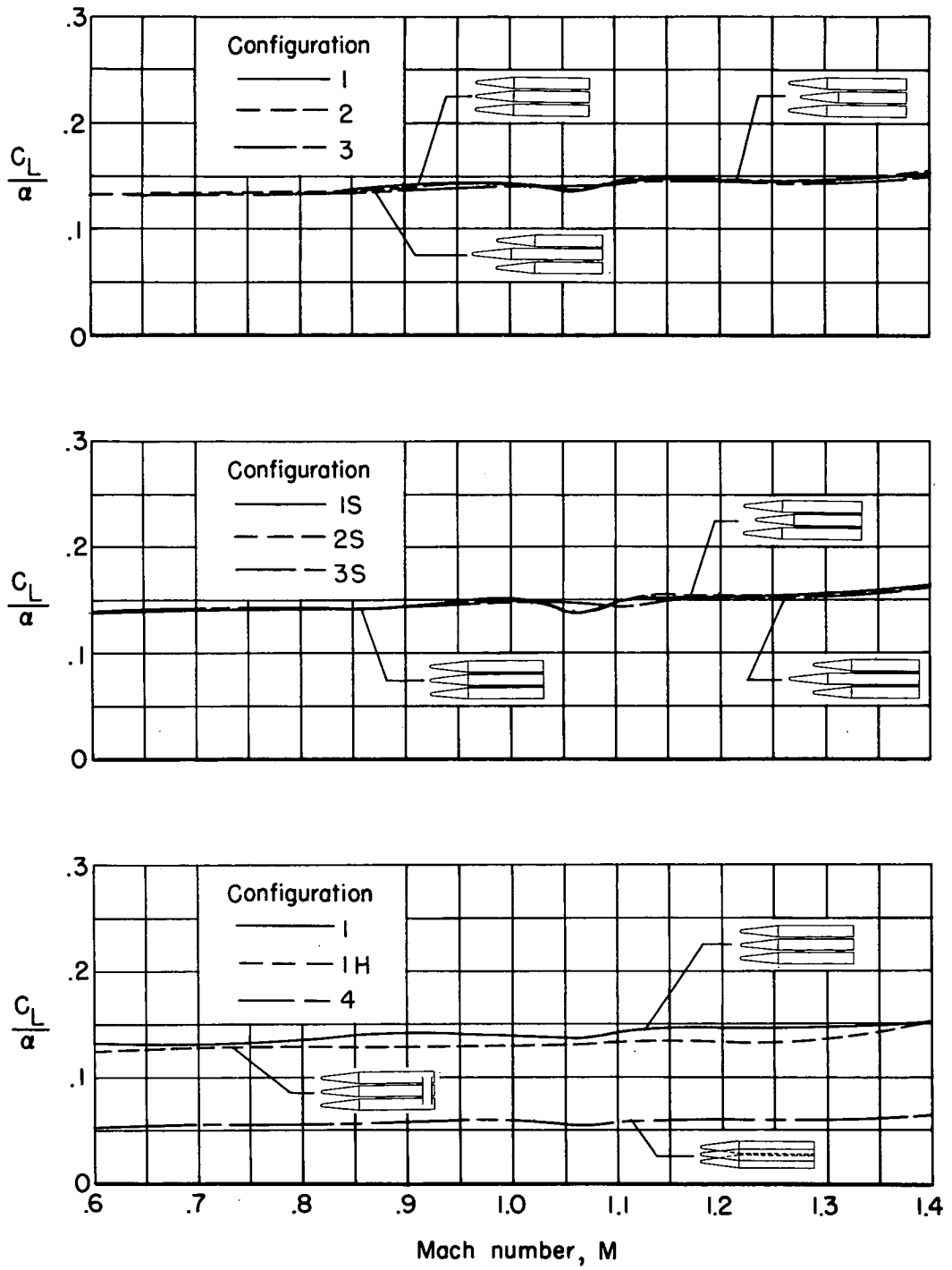

(c) $\alpha = 8°$

Figure 4. – Concluded.

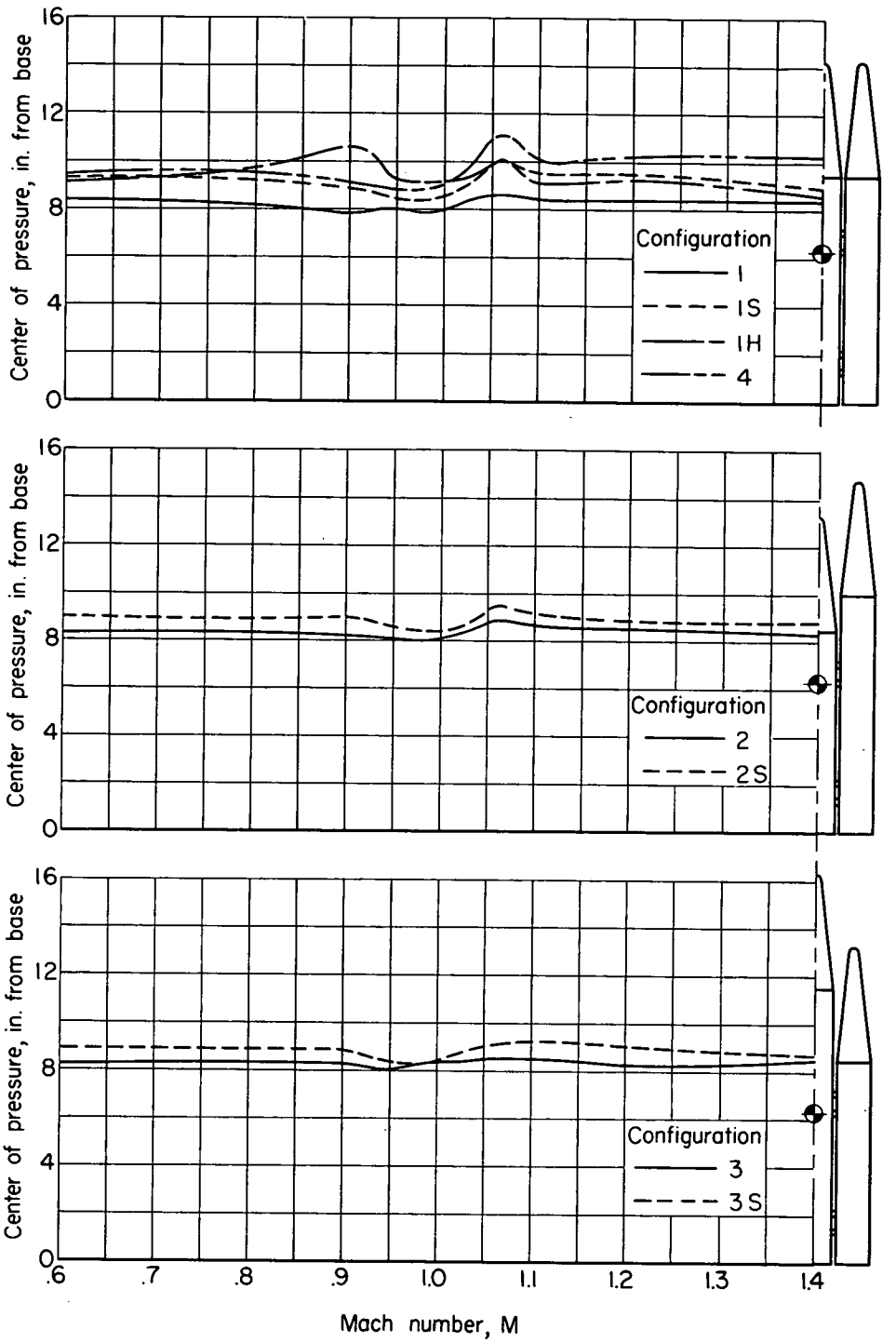

(a) $\alpha = 0°$

Figure 5.- Variation of center of pressure with Mach number for several triple-body missile configurations.

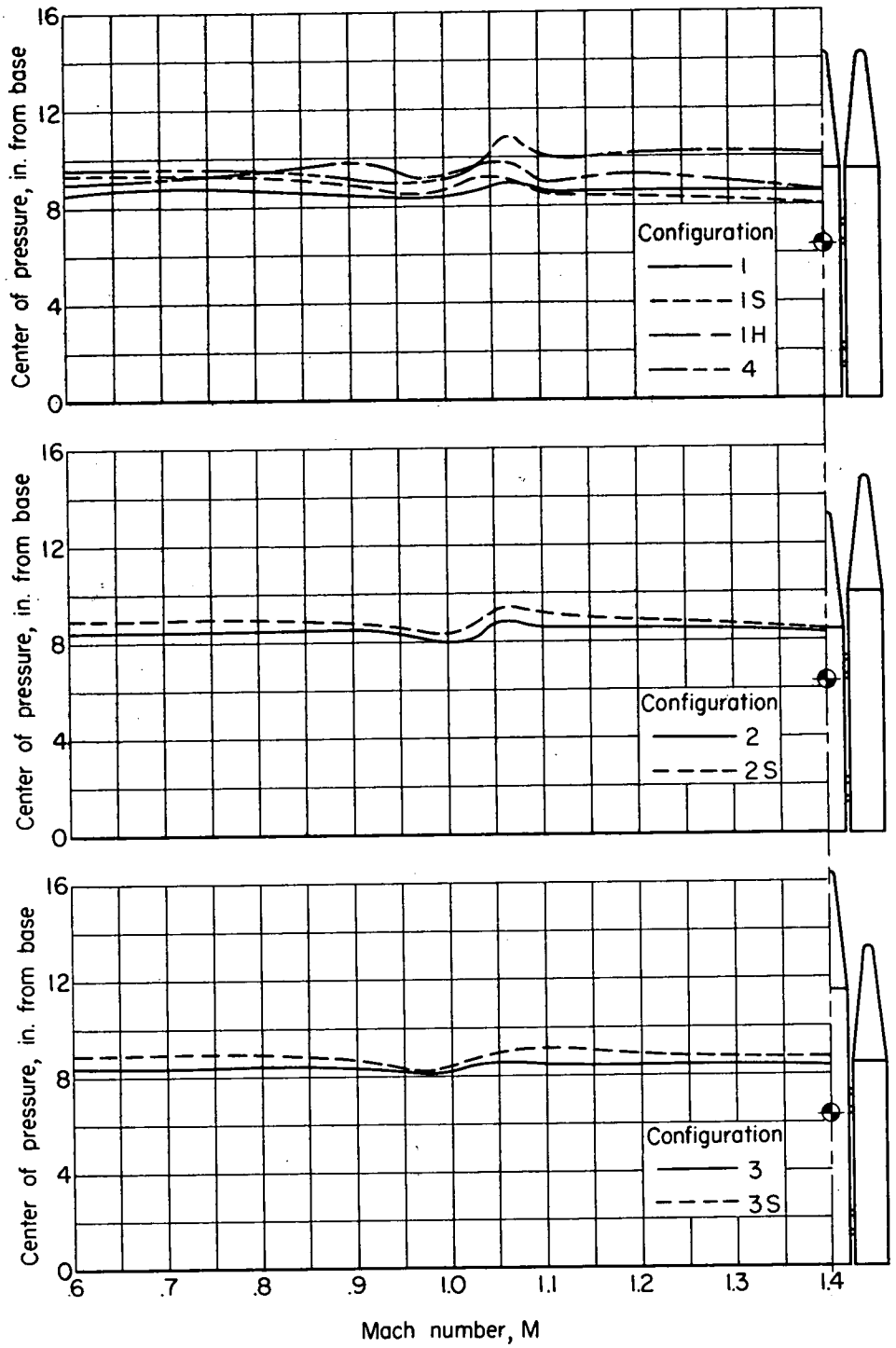

(b) $\alpha = 4°$

Figure 5. - Continued.

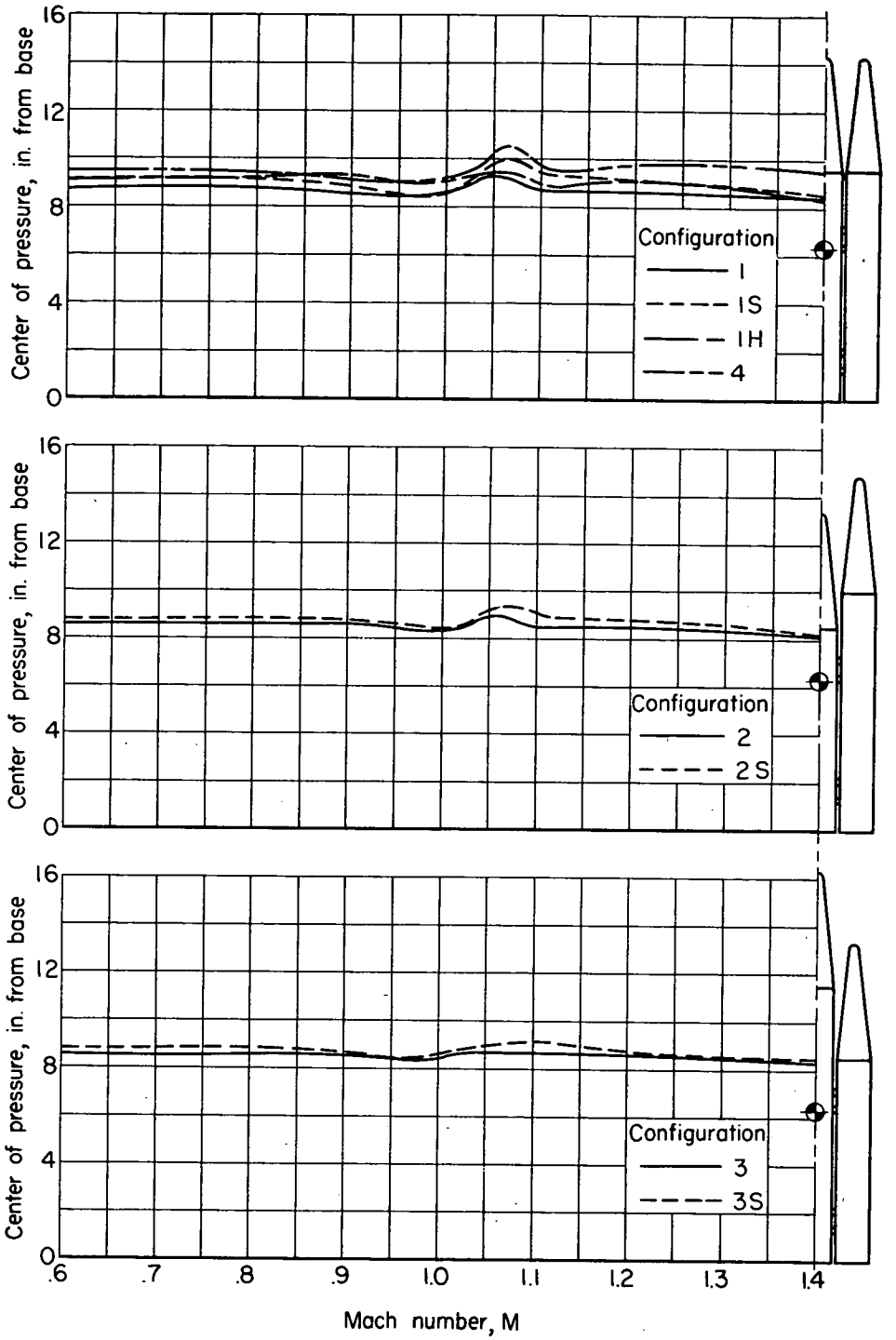

(c) $\alpha = 8°$

Figure 5.- Concluded.

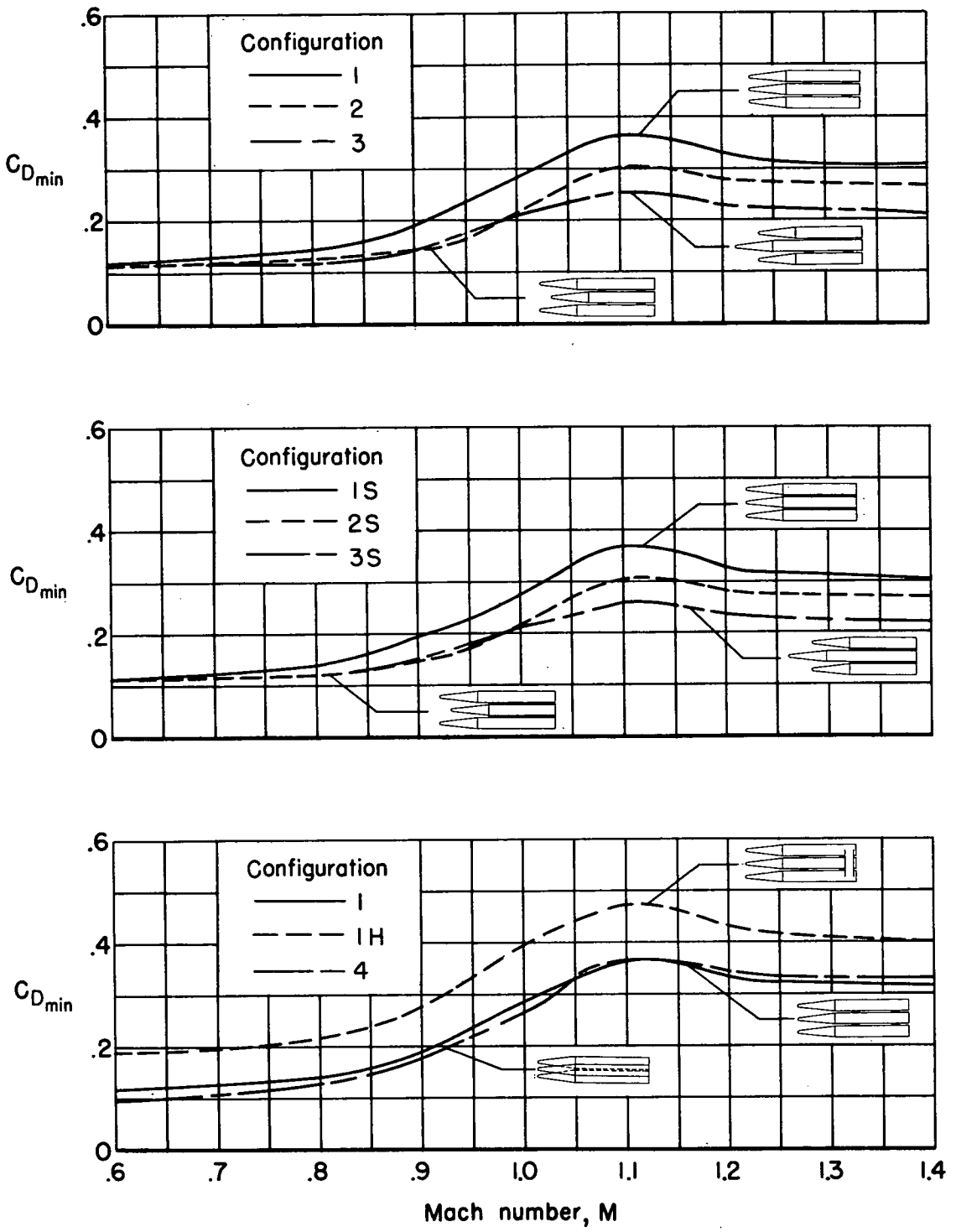

Figure 6. - Variation of minimum drag coefficient with Mach number for several triple-body missile configurations.

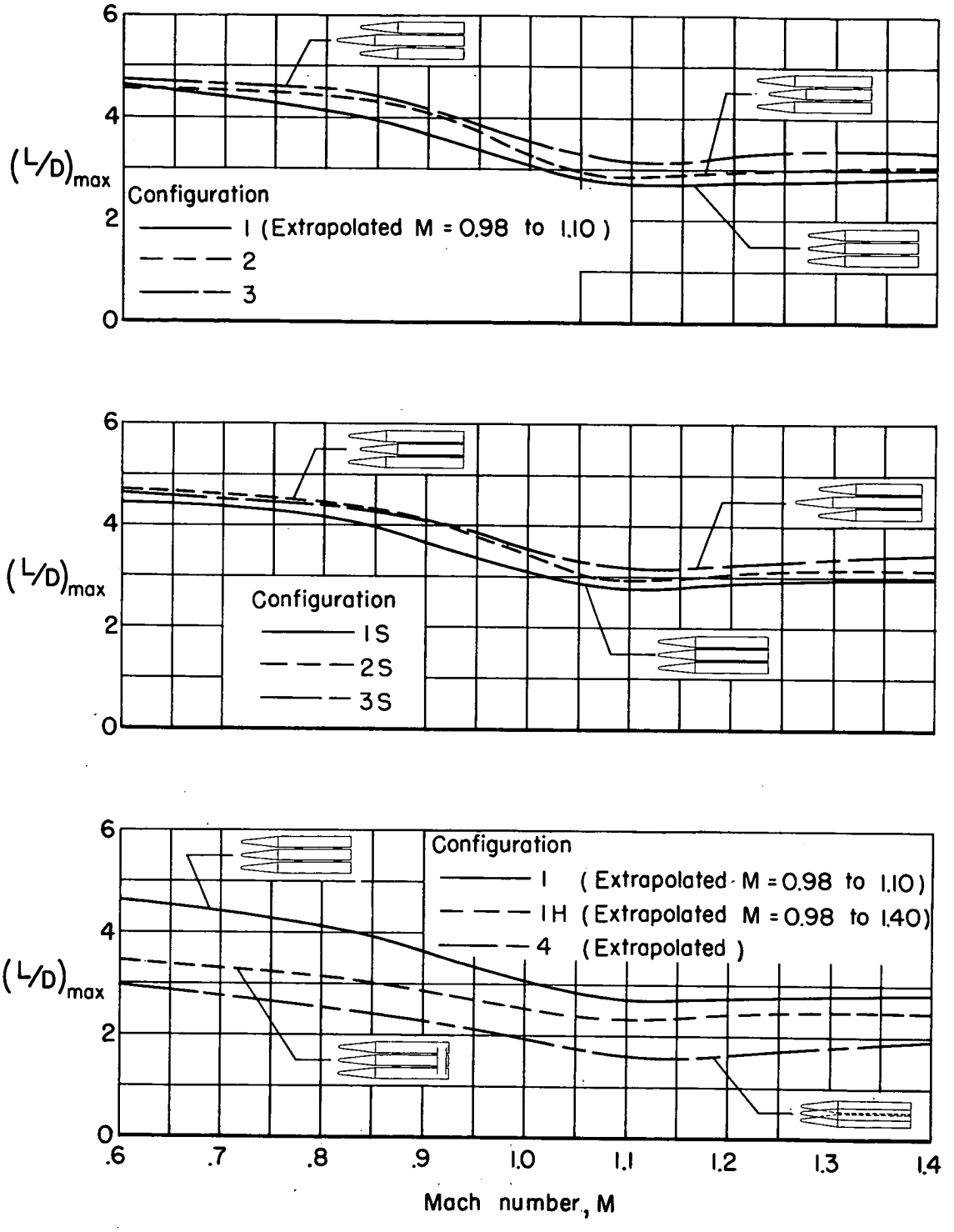

Figure 7. - Variation of maximum lift-drag ratio with Mach number for several triple-body missile configurations.

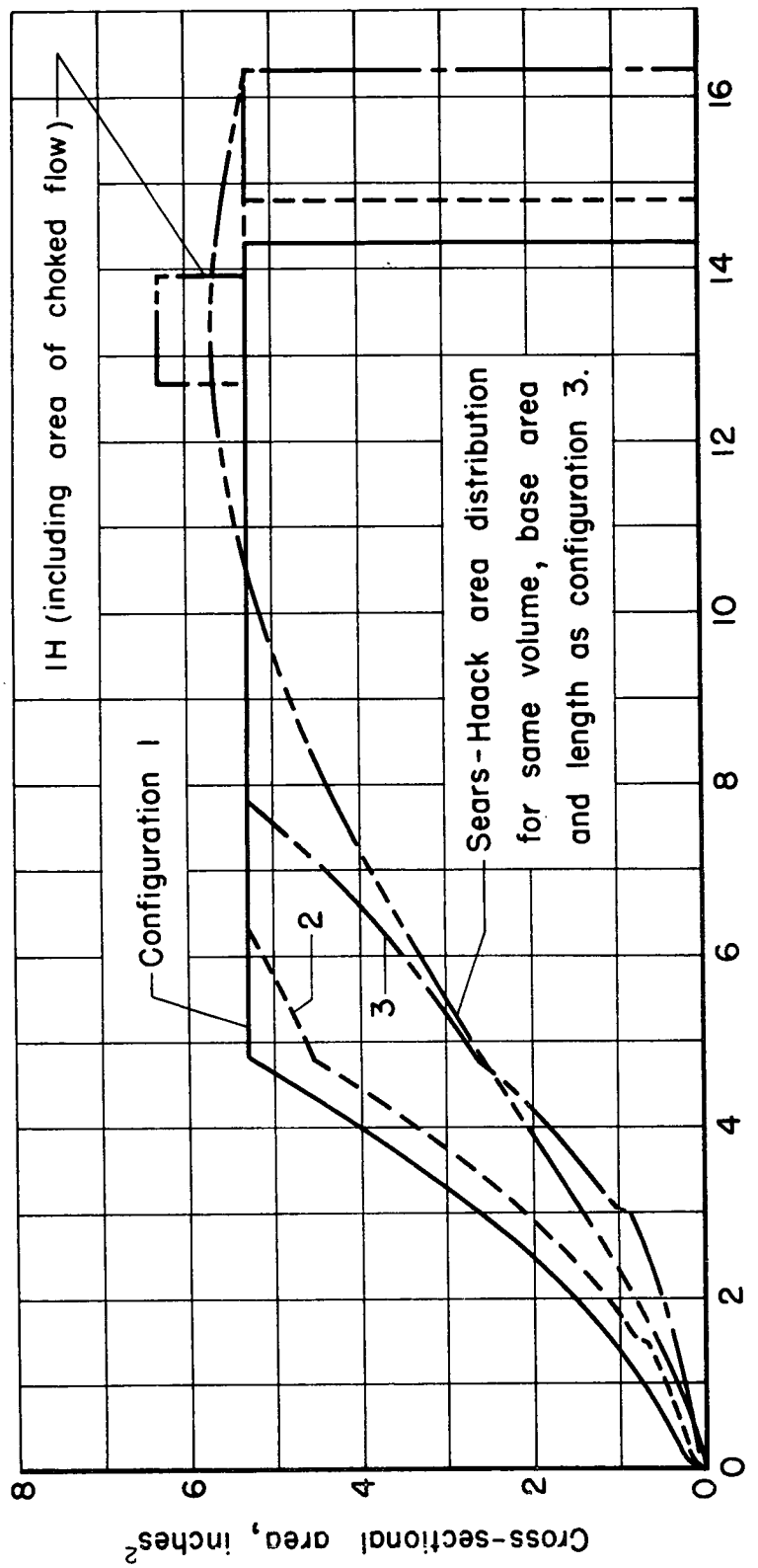

Figure 8.- Axial development of model cross-sectional areas for several triple-body missile configurations.

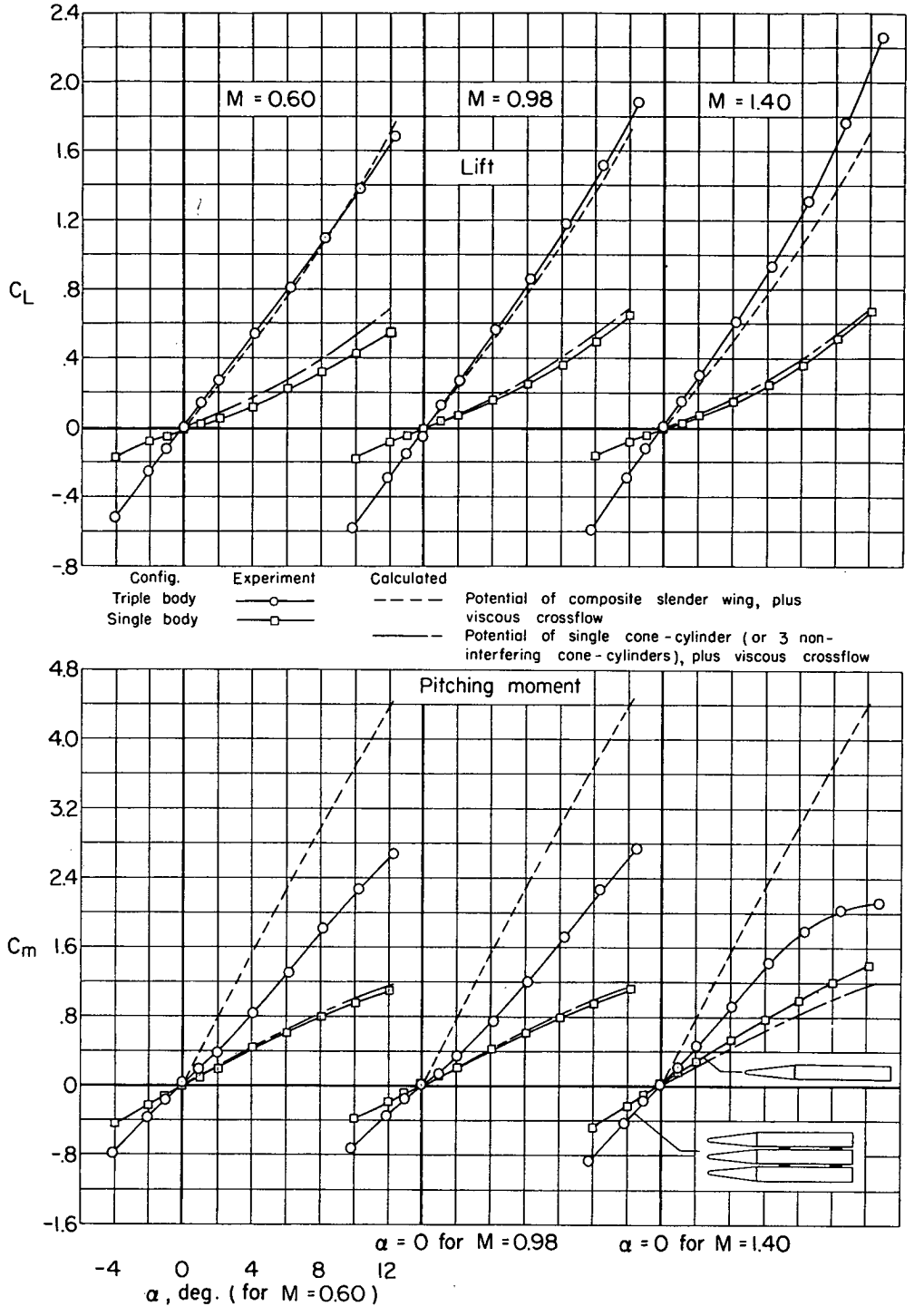

(a) Configuration 1.

Figure 9.- Comparison of experimental lift and pitching-moment with values calculated by various methods.

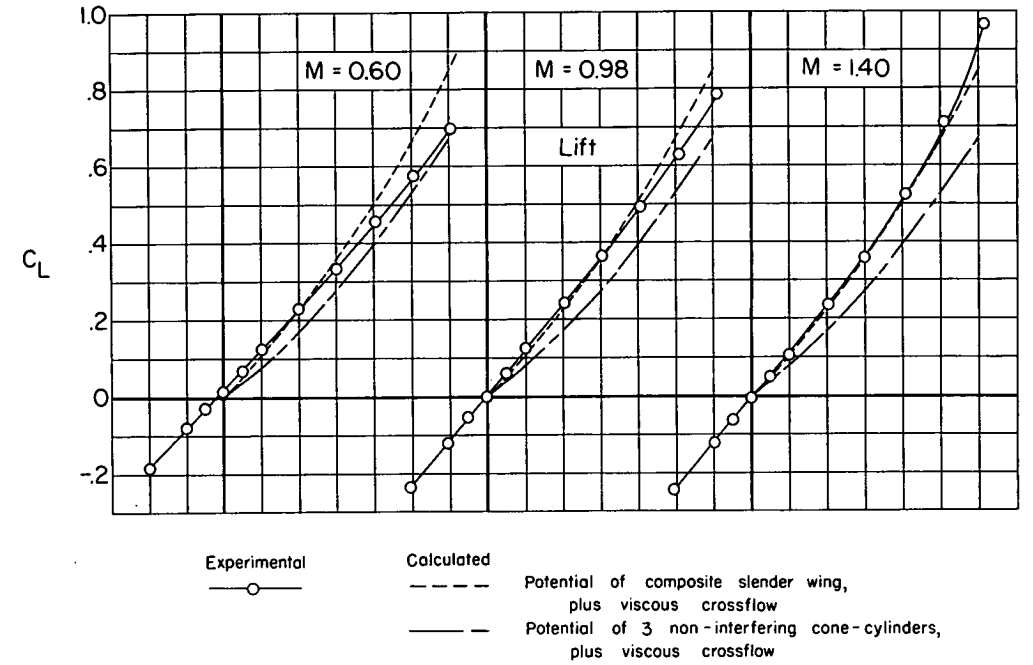

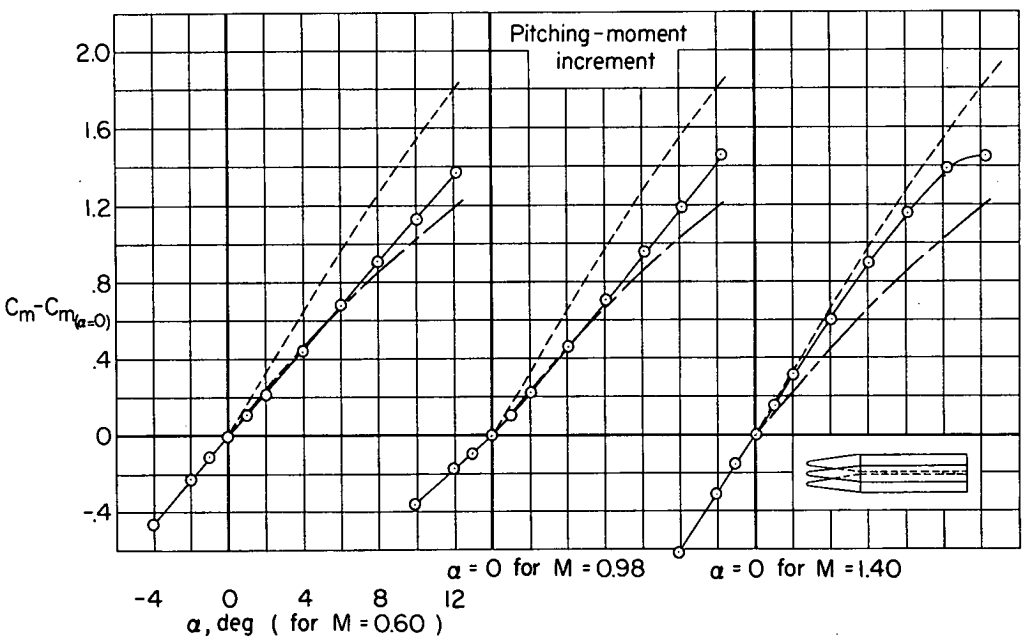

(b) Configuration 4.

Figure 9.- Concluded.